



How to improve the air quality over megacities in China: pollution characterization and source analysis in Shanghai before, during, and after the 2010 World Expo

K. Huang^{1,2}, G. Zhuang¹, Y. Lin¹, Q. Wang¹, J. S. Fu², Q. Fu³, T. Liu¹, and C. Deng¹

¹Center for Atmospheric Chemistry Study, Department of Environmental Science and Engineering, Fudan University, Shanghai, 200433, P. R. China

²Department of Civil and Environmental Engineering, The University of Tennessee, Knoxville, TN 37996, USA

³Shanghai Environmental Monitoring Center, Shanghai, 200030, P. R. China

Correspondence to: G. Zhuang (gzhuang@fudan.edu.cn), J. S. Fu (jsfu@utk.edu)

Received: 23 December 2012 – Published in Atmos. Chem. Phys. Discuss.: 6 February 2013

Revised: 27 April 2013 – Accepted: 23 May 2013 – Published: 20 June 2013

Abstract. Three field campaigns were conducted before, during, and after the 2010 World Expo in Shanghai, aiming to understand the response of secondary aerosol components to both control measures and human activities. In spring, PM_{2.5} (particulate matter) averaged $34.5 \pm 20.9 \mu\text{g m}^{-3}$ with a severe pollution episode influenced by a floating dust originating from northwestern China on 26–28 April, right before the opening of the expo. With the approaching expo a significant increasing trend of SNA (SO_4^{2-} , NO_3^- , and NH_4^+) concentrations was observed from 22 April to 2 May, attributed to the enhanced human activities. Nitrate had the most significant daily increasing rate of $1.1 \mu\text{g m}^{-3}\text{d}^{-1}$ due to enhanced vehicle emission. In summer, two intensive pollution episodes were found to be a mixed pollution of SNA with biomass burning due to loose control of post-harvest straw burning. In the autumn phase of the expo, before the closing of the expo (20–30 October), the air quality over Shanghai was much better than ever before. However, the air quality rapidly plummeted as soon as the expo was announced closed. SNA increased 3–6 fold to be 42.1 and $68.2 \mu\text{g m}^{-3}$ on 31 October and 1 November, respectively, as compared to 20–30 October. Of which, nitrate increased most ~ 5 – 8 fold, indicating the serious impact from enhanced vehicle emission. Compared to the spring and summer of 2009, NO_3^- increased 12–15 % while SO_4^{2-} showed reductions of 15–30 %. Continuous desulfurization of SO_2 emission from power plants in recent years was responsible for the lowered SO_4^{2-} , while increased traffic emission from the tremendous number of expo

visitors was the major contributor to the increased NO_3^- . Compared to the autumn of 2009, all the ion components increased in 2010, owing to the lifting of emission control measures after the expo. SO_4^{2-} was found least increased while NO_3^- and Ca^{2+} had tremendous increases of 150 and 320 %, respectively. The anthropogenic Ca as a tracer from construction dust increased from $2.88 \pm 1.85 \mu\text{g m}^{-3}$ during the expo to $6.98 \pm 3.19 \mu\text{g m}^{-3}$ during the post-expo period, attributed to the resumption of construction works after the expo. The lack of successive control measures with the loose regulations after the expo were responsible for this jump of the bad quality. The ratio of $\text{NO}_3^-/\text{SO}_4^{2-}$ in PM_{2.5} over Shanghai had a significant increasing trend from ~ 0.3 in the early 2000s to more than 1.0 in 2010, indicating the increasing role of mobile sources. Reducing NO_x emission will be China's priority in the future in order to improve the air quality over the megacities. In addition, lowering mineral aerosol components (e.g., Ca^{2+}) was also demonstrated to be beneficial for alleviating air pollution in China. This study demonstrated that stringent emission control measures aiming at mega-events in China could achieve positive benefits on improving the air quality in a short term. However, persistent efforts of curbing the anthropogenic emission remain a long way to go in the future.

1 Introduction

Shanghai hosted the 2010 World Expo from 1 May to 31 October, which was the most attractive mega-event in China after the 2008 Beijing Olympic Games. The six months long exhibition under the theme of “Better City Better Life” aimed to promote an environment-friendly and resource-saving “Green Expo”. A number of records were achieved during the expo. The number of countries and organizations that participated was the largest with more than 240 countries and international organizations. The number of volunteers was also the largest and the visitor numbers exceeded the target of 70 million, making the Shanghai Expo the biggest event in the World Expo history.

Air quality issue has always been a big concern and attracted tremendous attention in megacities of China, especially during some international mega-events. Lessons and experiences from the 2008 Beijing Olympic Games demonstrated the effect of unprecedented human perturbation on the large reductions of air pollution emissions and improvement of air quality (Wang et al., 2009, 2010). Different from the short-term Olympic Games, the Shanghai Expo extended a much longer time and hosted many more visitors, bringing more difficulties and challenges for ensuring the good air quality. Various long-term control measures were implemented during the 11th Five Year Plan (2006–2010), including implementation of stricter coal-fired boiler emission standards and clean fuel adoption, upgrade of the motor vehicles to National Standard IV, clampdowns on heavily polluting trucks, control of dust produced by construction operations, etc. (CAI-Asia, 2009). During the expo, additional measures were implemented. For instance, public transportation was encouraged as the primary means for travel. According to the circular of Shanghai Municipal People’s Government on restriction on transport of high-pollution vehicles, the vehicles within the inner-ring roads should have the environmental protection label. The exhaust emission of new cars must reach the national Class IV standard (equivalent to European IV standard) (cf. <http://en.expo2010.cn/a/20090605/000002.htm>). In addition, joint pollution controls over the Yangtze River delta (YRD) region (i.e., Shanghai, Jiangsu and Zhejiang provinces) were carried out to minimize the effect of regional transport on the air pollutants in Shanghai. Especially, the burning of straw was strictly prohibited (SEPB, 2010), which is a major source of air pollutants in the harvest season (Huang et al., 2012a).

The 2010 World Expo held in Shanghai provided a unique opportunity to analyze the impact of human-perturbed emission on air quality and advocate policy that will improve future air quality in Shanghai and in other Chinese cities. A space-based study showed a preliminary view of air quality in Shanghai and neighboring provinces, finding reductions of AOT (aerosol optical thickness), NO_2 , and CO in Shanghai during the expo period compared to the past three years. However, significant increases of NO_2 by 20 % and AOT by

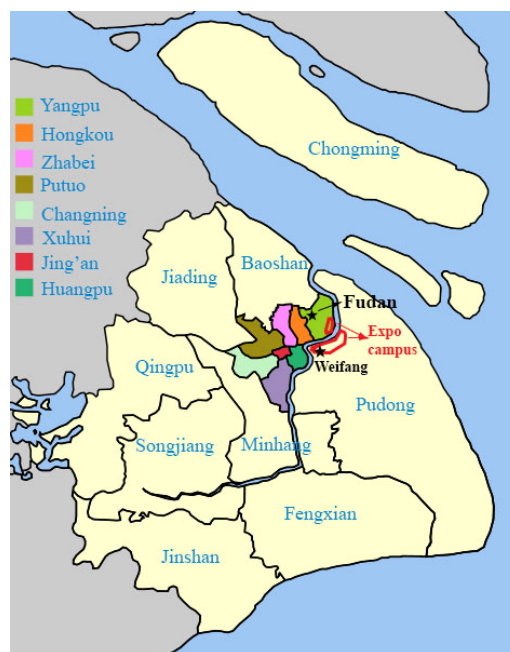


Fig. 1. Map of Shanghai with district borders. The area of the expo campus is shown by the red polygon, and the monitoring sites at Fudan and Weifang are denoted by the black stars (This figure is modified based on the map from <http://en.wikipedia.org/wiki/Shanghai>).

23 % over Shanghai urban areas were observed after the expo (Hao et al., 2011). A high-resolution time-of-flight aerosol mass spectrometer (HR-ToF-AMS) characterized the chemical composition of PM_{10} (particulate matter) in Shanghai during a less than 1 month study period of the expo (Huang et al., 2012c). However, a clear picture of potential impacts on air quality from human regulations during the expo remains ambiguous and is rarely interpreted.

The primary goal of this study is to obtain detailed information of the atmospheric chemical composition under the varied emissions during the expo. Three intensive field campaigns were performed during the three seasons that the expo spanned; namely 2 April–14 May in spring, 25 July–24 August in summer, and 20 October–29 November in autumn (Fig. 1). We specifically included some periods before and after the expo for comparison between the expo and non-expo periods. The atmospheric processing, source identification and formation mechanisms of selected pollution episodes are discussed on the basis of each season. Insights into the role of meteorology on air quality and response of atmospheric chemistry to anticipated emission variations are illustrated. In addition to the discussion of air quality during the expo, we also include results from 2009 for a detailed comparison to 2010.

2 Methodology

2.1 Field campaign

2.1.1 Observational site

Figure 1 shows the map of the Shanghai metropolitan area with district borders. The area of the expo campus is shown by the red polygon, partly built on the Pudong District and partly on the Yangpu District, which was separated by the Huangpu River. It occupied a total area of 5.28 km². The Fudan observational site (31.3° N, 121.5° E) was located in the Yangpu District as shown by the star in Fig. 1. The Fudan monitoring site was located to the northwest of the expo campus and the distance from the Fudan site to the expo campus was around 8–11 km. All the instruments were located on the roof (~20 m high) of a teaching building on the campus of Fudan University. Almost no high buildings are around this sampling site. This site could be regarded as representative of the megacity of Shanghai, standing for the mix of residential, traffic, construction, and industrial sources (Huang et al., 2012b). To verify whether the Fudan site can reflect the influences from the expo, we compare the PM₁₀ concentration of Fudan and that of the Weifang site (data source: SEMC (Shanghai Environment Monitoring Center)) inside the expo campus. As shown in Fig. S1a, the time series of PM₁₀ concentrations at these two sites co-varied very consistently with each other. Figure S1b shows the linear correlation of the hourly PM₁₀ concentrations between the two sites, with a significant correlation coefficient of 0.83. The slope of the regression equation reaches 0.97, very close to 1.00. Thus, this indicated the Fudan site could represent the air quality of the expo campus. Additionally, Fig. S2 shows the monthly wind rose at Fudan from May to October in 2010. Southeast winds dominated during the whole study period. Since the Fudan site was located to the northwest of the expo campus as shown in Fig. 1, it was evident that our monitoring site would be significantly impacted by the upstream emissions from the expo campus.

2.1.2 Automatic aerosol and gases monitoring

The Thermo Scientific TEOM 1405-D monitor simultaneously measured PM_{2.5}, PM-coarse (PM_{10–2.5}) and PM₁₀ mass concentration upon an oscillating balance. PM accumulated on a mounted filter. The accumulation of the PM mass caused the changes in the frequency of oscillation. And this frequency was detected in quasi-real time and then converted by a microprocessor into an equivalent PM mass concentration every few seconds and recorded in the running average of 10 min. The sampler split a PM₁₀ sample stream into its fine (PM_{2.5}) and coarse (PM_{10–2.5}) fractions using a USEPA (US Environmental Protection Agency) designed virtual impactor for the additional 2.5 μm cutpoint. The total flow rate operated at 16.67 L min⁻¹, and two sepa-

rate flow controllers maintained the coarse particle stream at 1.67 L min⁻¹ and the fine particle stream at 3.0 L min⁻¹. The instrument was operated at a temperature of 50 °C to avoid the interference of moisture on the calculation of aerosol concentrations. PM concentrations were averaged and used at intervals of 1 hr in this study. Trace gases instruments included a TECO 43i SO₂ analyzer, 49i O₃ analyzer, 48i CO analyzer, and a 42i NO-NO₂-NO_x analyzer. Some measures were implemented to eliminate the potential interference of NO_y species on NO₂ measurements as much as possible, for example, using filter and subtracting the concentration of HONO. A Teflon filter was placed in front of the Mo catalytic converter that connected to the gas sampler. The Teflon filter had a retention rate of over 99.7% for particles (e.g., particulate HNO₃) larger than 0.3 μm. The routine QA/QC (quality assurance/quality control) procedures included the daily zero/standard calibration, span and range check, station environmental control, staff certification, etc. according to the Technical Guideline of Automatic Stations of Ambient Air Quality in Shanghai based on the national specification HJ/T193–2005, which was developed following the technical guidance established by the U.S. Environmental Protection Agency (USEPA, 1998). The multi-point calibrations were weekly applied upon initial installation of the instruments and the two-point calibrations were applied on a daily basis.

2.1.3 Manual sampling

Aerosol samples of TSP (total suspended particles) and PM_{2.5} were collected on Whatman 41 filters (Whatman Inc., Maidstone, UK) using medium-volume samplers manufactured by Beijing Geological Instrument-Dickel Co., Ltd. (model: TSP/PM₁₀/PM_{2.5}; flow rate: 77.59 l min⁻¹). All the samplers were co-located with the online sampler. The duration time of sampling was generally 24 h. More samples with shorter duration times were collected during the heavily polluted days. The filters before and after sampling were weighed using an analytical balance (model: Sartorius 2004MP) with a reading precision 10 mg after stabilizing in constant temperature (20 ± 1 °C) and humidity (40 ± 1 %). All the procedures were strictly quality controlled to avoid the possible contamination of samples.

2.2 Chemical analysis

2.2.1 Ion analysis

One-fourth of each sample and blank filter was extracted ultrasonically by 10 mL deionized water (18 M Ω cm⁻¹). Eleven inorganic ions (SO₄²⁻, NO₃⁻, F⁻, Cl⁻, NO₂⁻, PO₄³⁻, NH₄⁺, Na⁺, K⁺, Ca²⁺, Mg²⁺) and four organic acids (formic, acetic, oxalic, and methylsulfonic acid (MSA)) were analyzed by ion chromatography (ICS 3000, Dionex), which consisted of a separation column (Dionex Ionpac AS 11), a guard column (Dionex Ionpac AG 11), a self-regenerating

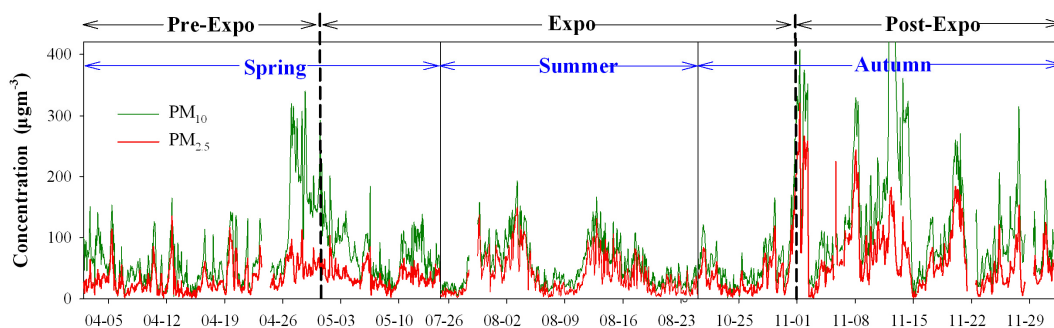


Fig. 2. Time series of hourly $\text{PM}_{2.5}$ and PM_{10} concentrations ($\mu\text{g m}^{-3}$) measured in Shanghai during 2010. The study period spans from spring (2 April–14 May) to summer (25 July–24 August) and autumn (20 October–29 November) as marked by the blue lines in the figure. Pre-expo (before 1 May) and post-expo (after 30 November) periods are separated from the expo period in the figure marked by the black lines.

suppressed conductivity detector (Dionex Ionpac ED50) and a gradient pump (Dionex Ionpac GP50). The detailed procedures are given in Yuan et al., 2003.

2.2.2 Element analysis

Half of each sample and blank filter was digested at 170°C for 4 h in high-pressure Teflon digestion vessel with 3 mL concentrated HNO_3 , 1 mL concentrated HCl , and 1 mL concentrated HF . After cooling, the solutions were dried, and then diluted to 10 mL with distilled deionized water. Total 24 elements (Al, Fe, Mn, Mg, Mo, Ti, Sc, Na, Ba, Sr, Sb, Ca, Co, Ni, Cu, Ge, Pb, P, K, Zn, Cd, V, S, and As) were measured by using an inductively coupled plasma atomic emission spectroscopy (ICP-OES; SPECTRO, Germany). The detailed analytical procedures are given in Sun et al., 2004; and Zhuang et al., 2001.

3 Results and discussion

3.1 Air quality of Shanghai when the expo was approaching

3.1.1 Pre-expo pollution: dust invasion

The spring phase of the field campaign included almost one month of the pre-expo period (2–30 April) and the first half of the opening expo month (1–14 May) as shown in Fig. 2. The average $\text{PM}_{2.5}$ and PM_{10} concentrations during this period were 34.5 ± 20.9 and $74.5 \pm 56.7 \mu\text{g m}^{-3}$, respectively. In the newly enacted Chinese Ambient Air Quality Standards (GB3095-2012), the Grade II standards for annual $\text{PM}_{2.5}$ and PM_{10} concentrations were set as 35 and $70 \mu\text{g m}^{-3}$, respectively. Based on this criterion, $\text{PM}_{2.5}$ concentration was below this standard while PM_{10} exceeded. Persistent emission controls during the past five years and additional control measures during the expo had made during the 2010 expo the best air quality period of the past decade in Shanghai (Lin et

al., 2012). The $\text{PM}_{2.5}/\text{PM}_{10}$ ratio had a moderate value of 50 % in this period; because eastern China is frequently influenced by the floating dust originating from the deserts in northern and western China in spring (Huang et al., 2010, 2012a; Wang et al., 2007).

From 2 to 25 April, particle concentrations generally stayed at low levels with several small peaks occurring occasionally. The mean concentrations of $\text{PM}_{2.5}$ and PM_{10} during this period were 28.9 ± 21.4 and $52.8 \pm 32.6 \mu\text{g m}^{-3}$. However, a high pollution episode happened after this clean period. Starting from 15:00 LST (local standard time) on April 26, particle concentrations sharply climbed up with hourly peaks of over $300 \mu\text{g m}^{-3}$. Heavy pollution lasted till 28 April. Afterwards, particle concentrations, especially PM_{10} , started to decrease quickly. As this pollution occurred right before the opening of the expo, we denoted it as the “pre-expo pollution”. During this period, $\text{PM}_{2.5}$ and PM_{10} averaged 58.0 and $191.8 \mu\text{g m}^{-3}$, respectively. Compared to the previous period (i.e., April 2 to 25), $\text{PM}_{2.5}$ increased about 1 fold while PM_{10} increased almost 3 fold with a low $\text{PM}_{2.5}/\text{PM}_{10}$ ratio of 0.30. Hence, this pre-expo pollution was evidently caused by coarse particles. Figure 3b shows the daily Al concentrations in the total suspended particles (Al_{TSP}) along with the hourly PM_{10} concentrations during the spring of 2010. Al is a good trace element for mineral aerosol and its abundance could be used to quantify the intensity of the mineral source. Corresponding to the high pollution on 26–28 April, Al_{TSP} also presented very consistent high peaks and temporal variation with that of PM_{10} . The average Al_{TSP} during the pre-expo pollution episode reached $16.2 \mu\text{g m}^{-3}$. To quantify the mass concentration of mineral aerosol, it could be estimated by summing the major mineral elements with oxygen for their normal oxides, by using the formula: $[\text{Mineral concentration}] = 2.2[\text{Al}] + 2.49[\text{Si}] + 1.63[\text{Ca}] + 2.42[\text{Fe}] + 1.94[\text{Ti}]$ (Malm et al., 1994). Hence, the mineral aerosol during the pre-expo pollution episode accounted for a dominant mass fraction of 69 % in TSP. Figure S3 illustrates the

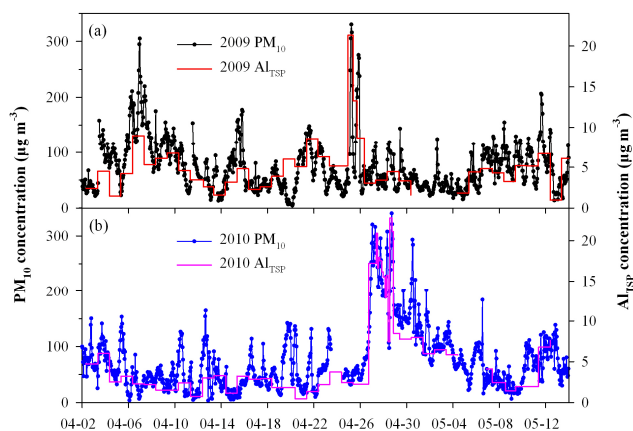


Fig. 3. Time series of hourly PM_{10} concentrations and daily Al concentrations in TSP (Al_{TSP}) during the spring study period from 2 April to 12 May in 2009 (a) and 2010 (b), respectively.

cluster of three-day back trajectories ending at Shanghai and the average MODIS (Moderate Resolution Imaging Spectroradiometer) deep blue AOD (aerosol optical depth) at 550 nm during this episode. It clearly shows high AOD hotspots over the dust source regions of China, i.e., the Gobi Desert in Mongolia/Inner Mongolia, and the Taklimakan Desert. The transport pathways from the back trajectories corroborated that this pre-expo pollution was caused by the dust intrusion.

Compared to the same study period in 2009 (Fig. 3a), we also observed a floating dust event at the end of April. On April 25 in 2009, the daily Al_{TSP} reached $13.7 \mu\text{g m}^{-3}$ and the mineral aerosol accounted for 76.8 % of TSP. This pollution had been investigated and determined to originate from the Gobi Desert (Huang et al., 2012a). Similar meteorological conditions on the dusty days were observed. As shown in Fig. 4a, b and d, e, the two dust events in 2010 and 2009 both occurred in specific meteorological conditions, e.g., prevailing northwesterlies, reduced dew points and low humidity. The prevalence of the Mongolian anticyclone originating from Mongolia and northern China triggered dust events frequently in spring. The intrusion of dust aerosol was not accidental and could be a potential threat to the air quality of the downstream regions.

If the dust events were excluded in both years, the average Al_{TSP} concentration in the spring of 2009 and 2010 were 4.25 ± 1.89 and $3.48 \pm 2.11 \mu\text{g m}^{-3}$, respectively. Approximate 20 % reduction of the mineral dust was found in 2010. In megacities of China, mineral dust mainly derived from construction works and re-suspended road dust. In order to alleviate the dust emission, the Shanghai government banned most construction sites, implemented various dust-proof measures, and cleaned the roadsides regularly, etc. It was estimated that construction dust dropped by 29 % during the expo (CAI-Asia, 2011). This indicated that the special regulations did help to reduce the emission of local dust and

explained the lower mineral aerosol concentrations in 2010 than in 2009.

3.1.2 Response of secondary aerosol to human activities

Figure 4 shows the daily concentrations of major secondary inorganic aerosol (SNA, i.e., SO_4^{2-} , NO_3^- and NH_4^+) in $\text{PM}_{2.5}$ with meteorological parameters (wind speed/direction, temperature, dew point, precipitation, relative humidity and atmospheric pressure) during the spring of both 2010 and 2009. Comparison between the temporal variations of SNA in these two years illustrated that intensive pollution episodes occurred in completely different time frames. In the spring of 2009, one intensive pollution episode occurred from 4 to 10 April with average SNA concentration of $48.86 \pm 5.01 \mu\text{g m}^{-3}$, which had been investigated to be related to the local anthropogenic emission (Huang et al., 2012a). During the same period in 2010, SNA concentration was about 70 % lower. Wind speed could be a major factor responsible for this difference as it was higher in 2010 (mean: 3.0 ms^{-1}) than that in 2009 (mean: 2.4 ms^{-1}). Additionally, air masses from 4 to 10 April in 2010 predominantly came from the northeast and southeast over the East China Sea, facilitating the dispersion of air pollutants. Apart from the high pollution episode in 2009, SNA stayed at relatively low levels of $10.9 \pm 4.7 \mu\text{g m}^{-3}$ during the remaining days. However, the situation became the opposite in 2010. Mean SNA concentration from 11 April to 14 May in 2010 was $15.4 \pm 8.4 \mu\text{g m}^{-3}$, about 40 % higher than 2009. No significant differences were found among the major meteorological parameters except precipitation in these two years since 11 April (Fig. 4a, b, d, e). Although more precipitation events occurred since April 11 in the spring of 2010 (e.g., on 11, 13–14, and 20–21 April) than in the same period of 2009 (note that no aerosol was sampled on 19 and 24 April when intense precipitation events occurred), the mean SNA level was still found higher than in 2009 as discussed above. This suggested that the anthropogenic emission was enhanced as the expo was approaching. Since 22 April in 2010, rare precipitation events occurred and the role of wet scavenging on cleansing the air pollutants was negligible. The temporal variation of SNA presented an evidently increasing trend from 22 April to 2 May in 2010 (Fig. S4). Although temperature gradually increased during this period and higher temperature did not favor the accumulation of nitrate and ammonium in the particulate phase, nitrate still had significant increase from $4.0 \mu\text{g m}^{-3}$ on 22 April to $13.4 \mu\text{g m}^{-3}$ on 2 May with a peak value of $18.0 \mu\text{g m}^{-3}$ on 29 April. The daily increasing rate of nitrate during this period reached $1.1 \mu\text{g m}^{-3} \text{ d}^{-1}$ with a linear correlation coefficient of 0.9. The $\text{NO}_3^-/\text{PM}_{2.5}$ ratio increased from 13.5 % on 22 April to 31.3 % on 2 May, indicating the role of NO_3^- in the atmospheric processing became more and more important. This should be related to the enhanced traffic emission due to the increasing visitor numbers. Sulfate also had an obvious increasing trend with an

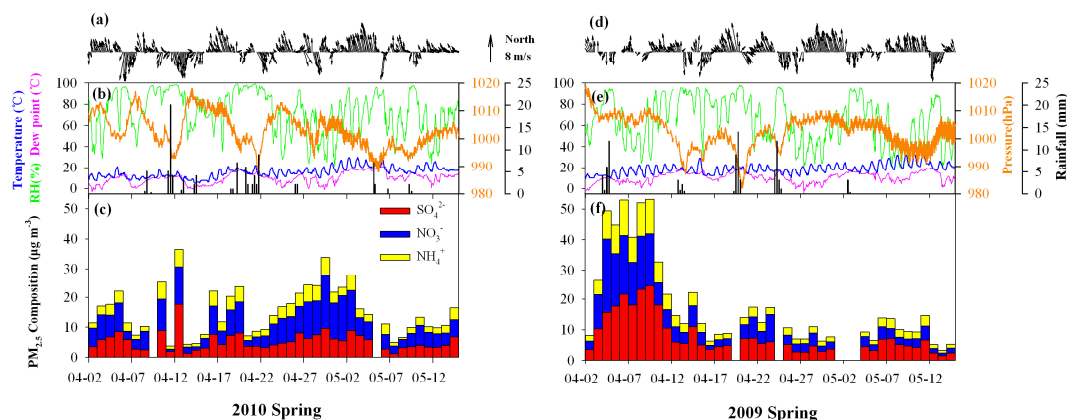


Fig. 4. (a and d) Hourly wind speed/direction; (b and e) atmospheric pressure, relative humidity, dew point, temperature, and precipitation; (c and f) daily PM_{2.5} inorganic secondary composition (i.e., SO₄²⁻, NO₃⁻ and NH₄⁺) concentrations during the spring in 2010 and 2009, respectively.

increasing rate of $0.41 \mu\text{g m}^{-3} \text{d}^{-1}$, which was probably due to the increasing electricity demand. In regard of the high pollution on 29 April, there was a mandatory abatement of power plants emissions afterwards and around 30 % of SO₂ emission was reduced to ensure the recovery of air quality in the next few days (SEMC, 2011). It was observed that the air quality was alleviated to some extent on April 30, indicating the emission reduction was effective. However, SNA concentrations rose again in the first two days of the expo (May 1 and 2) although meteorological conditions were favorable, e.g., southeast winds from the ocean and high wind speeds (Fig. 4a). Figure S5 shows the daily numbers of the expo visitors from 1 to 14 May. The temporal variations of SNA since the opening of the expo corresponded well with that of visitor numbers, suggesting the human activities can be a major factor affecting the pollution level. On 1 and 2 May, visitor numbers both exceeded 200,000, which were at high levels in this study period, and could explain the high SNA level on these two days. Afterwards, the daily visitor numbers from 3 to 7 May decreased about 40 %. It was found that several rainfall events occurred on 5 and 6 May, and this probably partly accounted for the lower attendance number. Both reduced expo visitors and the occurrences of precipitation were beneficial for the reduction of air pollution, which was reflected in the decrease of PM concentrations (Fig. 2) and also the SNA concentrations (Fig. 4c). After that, there was an increasing trend of expo visitors and slightly increasing SNA concentrations were also observed. Overall, we found out human activities dominated the variations of aerosol chemistry in the spring phase of the expo.

3.2 Expo in summer: biomass burning pollution

The summer phase of the expo study period lasted from 25 July to 24 August. After almost three months of operation, the daily visitor numbers of the expo became relatively

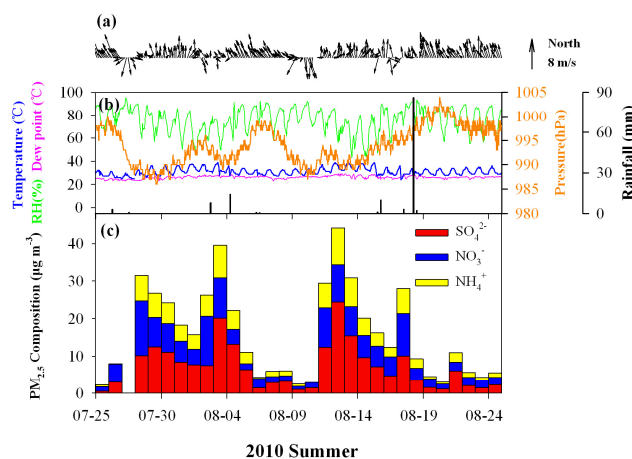


Fig. 5. Same as Fig. 4 but for the summer of 2010.

steady with a daily number of around 42 000. During this period, the major meteorological conditions fluctuated insignificantly. For example, the standard deviation of temperature, dew point, RH (relative humidity), and atmospheric pressure was $3.1 \text{ }^\circ\text{C}$, $1.2 \text{ }^\circ\text{C}$, 10.7% , and 3.9 mb , respectively, as compared to their average values of $31.1 \text{ }^\circ\text{C}$, $26.1 \text{ }^\circ\text{C}$, 75.8% , and 994.0 mb . Winds predominantly blew from the southeast as shown in Fig. 5a. Precipitation events occurred mainly on four days, i.e., on 2, 4, 15, and 18 August. The wet scavenging would generally reduce the aerosol concentrations, especially the heavy rain on 18 August caused a significant decrease of SNA levels as shown in Fig. 5c. The average PM_{2.5} and PM₁₀ concentrations during this period were 37.5 ± 30.9 and $56.6 \pm 37.1 \mu\text{g m}^{-3}$, respectively. Compared to spring, PM_{2.5} was higher while PM₁₀ decreased a lot. Higher humidity and the absence of dust events during summer should be the major reasons for the lower coarse-particle concentrations. Particle concentrations fluctuated significantly, and

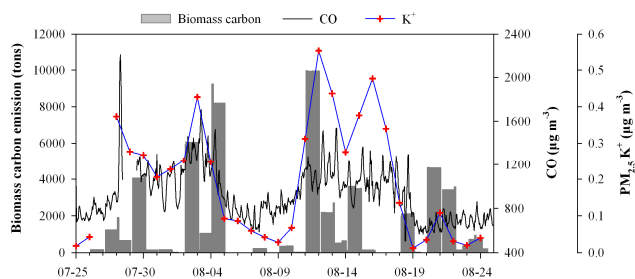


Fig. 6. Hourly CO concentration ($\mu\text{g m}^{-3}$), hourly biomass carbon emission (tons h^{-1}) from the FLAMBE biomass burning emission inventory in the domain of $28\text{--}32^\circ\text{ N}$, $119\text{--}123^\circ\text{ E}$ in eastern China with daily K^+ concentration in $\text{PM}_{2.5}$ during the summer of 2010.

two intensive pollution episodes were observed, one from 28 July to 4 August, and the other from 11 to 17 August (Figs. 2, 5c). In this period, meteorologic conditions did not vary much (Fig. 5a, b), indicating the fluctuation of air quality was more emission driven. Overall, SNA contributed a moderate fraction of 40 % to $\text{PM}_{2.5}$ and mineral aerosol contributed less than 10 %, leaving a significant fraction of particle mass unexplained. The Pearson linear correlations between SO_2 , NO_2 , CO and $\text{PM}_{2.5}$ were plotted for each study period in Fig. S6. In summer, SO_2 showed weak correlation with $\text{PM}_{2.5}$ (correlation coefficient $R = 0.47$) and NO_2 showed moderate correlation ($R = 0.66$), while CO showed the most significant correlation with $\text{PM}_{2.5}$ ($R = 0.76$). This meant that anthropogenic emission was not the dominating source of air pollution. The highest correlation between CO and $\text{PM}_{2.5}$ was typically observed during biomass burning events as CO was a major product from incomplete combustion of biomass (Huang et al., 2012a; Sun et al., 2009). Figure 6 shows the time series of hourly CO and daily particulate K^+ concentrations. These two species varied very consistently with each other and both increased during the two intensive episodes. K^+ was a typical tracer for biomass burning and its concurrent temporal variation with CO, $\text{PM}_{2.5}$, and PM_{10} suggested that biomass burning was indeed a considerable source for the two intensive episodes during summer. MODIS detected intense fires burning over the Yangtze River delta region as shown by the fire spots in Fig. S7. During the first pollution episode (28 July to 4 August), considerable numbers of fire spots were distributed over the majority area of the Yangtze River delta, especially in the central and southern part of Jiangsu Province, and northern part of Zhejiang Province. For the second pollution episode (11 to 17 August), although the total numbers of fire spots reduced a lot compared to the first one, the Shanghai metropolitan area was still surrounded by intense biomass burning from neighboring provinces, i.e., northern Zhejiang and part of Jiangsu Province. Facilitated by the prevailing southeast winds (Fig. 5a), air quality of Shanghai could be indeed impacted by biomass burning from the neighboring regions. From a high resolution biomass burning emission inventory

FLAMBE (Fire Locating and Modeling of Burning Emissions, (Reid et al., 2009)), we calculated the hourly biomass carbon emission in the domain of $28\text{--}32^\circ\text{ N}$, $119\text{--}123^\circ\text{ E}$ and presented its temporal variation in Fig. 6. The intensity of biomass carbon emission co-varied relatively well with CO and K^+ concentrations, further corroborating the impact of biomass burning on the local air quality.

Summer is the main harvest season in eastern China. Farmers were busy during the harvest, with substantial production of crop residues. Callback or recycling use of these biofuels was costly, while the most convenient way to get rid of the crop residues was to burn them (Yang et al., 2008). Although Shanghai, Jiangsu and Zhejiang governments jointly issued the announcement on prohibiting the open burning of crop residues during the expo (SEPB, 2010), the results in this study indicated that considerable and widespread biomass burning still occurred. On the one hand, unpredictable human activities on biofuel combustion and the sparse distribution of biomass emissions increased the difficulty of preventing the occurrence of biomass burning. On the other hand, regulation enforcement in most Chinese local governments was not good enough, especially in some remote counties. Also, due to the lack of common sense of environmental protection, some farmers did not obey the regulations and just burned the crop residues privately.

3.3 Rebound of poor air quality: post-expo pollution

3.3.1 Deterioration of air quality on the closing day of the expo

As the expo approached its end, more visitors sought the last chance to visit it, causing October to be the busiest month contributing over 20 % of the total visitor numbers during the whole expo. Air quality was monitored from 20 October to the close of the expo on 31 October with continuous measurement till 2 December. As shown in Fig. 2, a notable change of air quality between the two time frames was observed. From 20 to 30 October before the close of the expo, $\text{PM}_{2.5}$ and PM_{10} averaged 30.6 and $51.3 \mu\text{g m}^{-3}$. Other pollutants, for example, SO_2 , NO_2 and CO averaged 19.1 , 41.2 , and $821.4 \mu\text{g m}^{-3}$, respectively. The air quality in Shanghai during this period could be regarded as “good” and we believed that stringent control measures must be implemented to keep the air quality “good”. In addition, Shanghai experienced strong northerly winds from 20 to 30 October (Fig. 8a) and this also contributed to the better air quality. However, all the air pollutants drastically increased during the day (31 October) when the expo was announced to be closed. Figure 7 shows the diurnal variation of $\text{PM}_{2.5}$, PM_{10} , NO_2 , CO, and SO_2 with an hourly wind profile from 30 October to 2 November. No precipitation events were observed during this period. On 30 October, the concentrations of all the air pollutants stayed at a relatively low level. Strong wind was partly responsible for this. From 00:00 LST on 31 October,

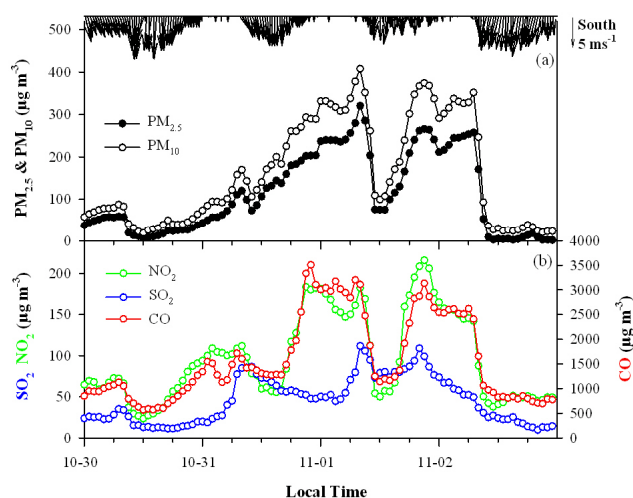


Fig. 7. Time series of hourly (a) particles ($\text{PM}_{2.5}$, PM_{10}) and (b) pollutant gases (NO_2 , SO_2 , CO) concentrations from 30 October to 2 November 2010.

$\text{PM}_{2.5}$ and PM_{10} concentrations gradually increased till the early morning of the next day. Although stronger winds appeared from around 09:00 to 20:00 LST on 31 October, the concentrations of air pollutants did not decrease and instead continued to increase, suggesting an increase of local emissions. From 20:00 LST to the next morning, the atmosphere turned to be stagnant as indicated by the absence of winds. $\text{PM}_{2.5}$ and PM_{10} continued to rise and reached the extremely high concentrations of 320.8 and 407.8 $\mu\text{g m}^{-3}$ at 08:00 LST of 1 November. Afterwards, PM concentrations sharply decreased and reached troughs around noon. The appearance of northeast and north winds evidently was beneficial for cleaning the air pollution. In addition, the elevated mixing layer at noon due to higher temperature could also dilute the emission. However, PM climbed up again and stayed at high levels till 07:00 LST on 2 November. Afterwards, persistent northeast and north winds from the ocean helped cleanse the air of pollutants again. During these four days, insignificant differences of wind pattern, temperature, atmospheric pressure, relative humidity and dew point were observed. However, compared to the reference period of 30 October, completely different diurnal patterns and concentrations of air pollutants in the following days were observed. Enhanced local emission was suggested to be mainly responsible for this tremendous rebound of all the air pollutants. This clearly indicated the lifting of short-term emission control measures (e.g., loose control on the vehicle flows, and allowance of high-duty vehicles into the city) that took place right after the announcement of the closing of the expo.

The temporal variations of pollution gases could probably give us some clues on the pollution source. Figure 7b shows that NO_2 and CO varied very consistently and showed peaks as those of particles around the same time. NO_2 and CO both started to climb very quickly at 17:00 LST on 31 October

and reached over 150 and 2500 $\mu\text{g m}^{-3}$, respectively, lasting almost 14 h till 09:00 LST on 1 November. Another similar pollution episode started at 16:00 LST on 1 November and ended at 07:00 LST on 2 November. Mean NO_2 and CO concentrations reached 104.5 and 1715.8 $\mu\text{g m}^{-3}$ on 31 October, and 144.5 and 2398.9 $\mu\text{g m}^{-3}$ on 1 November, respectively. The NO_2 level even exceeded that of the ever recorded heaviest pollution in Shanghai on January 19, 2007 (Fu et al., 2008). NO_2 and CO both significantly correlated with $\text{PM}_{2.5}$ with correlation coefficients of 0.81 and 0.88 during this pollution episode, respectively. Fire spots detected from MODIS on Aqua and Terra satellites on 31 October and 1 November are plotted in Fig. S8. Almost no or very few fire spots were observed in Shanghai and areas adjacent to Shanghai. Thus, the possible impact of biomass burning emission on the extremely high CO and NO_x concentrations could be neglected. The peak occurrences of NO_2 and CO during the rush hours indicated traffic emission should be one of the main causes for the deterioration of air quality near the end of the expo and after the expo. Although the SO_2 concentration during this period also increased compared to during the expo, its temporal variation did not fluctuate as strongly as that of NO_2 and CO as shown in Fig. 7b. Also, the linear relationship between SO_2 and $\text{PM}_{2.5}$ only presented a moderate correlation coefficient of 0.42. This indicated that stationary sources (e.g., power plants, industrial emission) were not the dominant contributors to this heavy pollution.

Owing to the significant enhanced pollutant precursors, the corresponding increase of SNA was expected as shown in Fig. 8c. SNA in $\text{PM}_{2.5}$ reached 42.1 and 68.2 $\mu\text{g m}^{-3}$ on 31 October and 1 November, respectively. Compared to 20–30 October, SNA increased 3–6 fold. Of which, nitrate increased the most, about 5–8 fold, while sulfate and ammonium increased about 2.5–4.5 fold. Among the total water soluble inorganic ions, nitrate accounted for the largest fraction of 50%, corroborating the impact from the enhanced vehicle emission. Overall, air quality in Shanghai had plummeted since the expo was announced closed, sliding from “good” to “severely polluted”.

3.3.2 Other secondary inorganic pollution episodes

Compared to the spring and summer study periods, much more occurrences of intensive pollution episodes and higher pollution peaks were observed during the post-expo period as shown in Fig. 2. Except for the heavy pollution episode discussed above, there were also several other secondary inorganic pollution episodes as shown in Fig. 8c. Three SNA pollution episodes were sorted out, which occurred on 6–7, 19–21 November, and 1–2 December. The average SNA concentration during these episodes reached 46.9 $\mu\text{g m}^{-3}$ and accounted for 55% of $\text{PM}_{2.5}$. The three pollutant gases (i.e., SO_2 , NO_2 and CO) all presented significant correlations with $\text{PM}_{2.5}$, which were the highest during the three study periods (Fig. S6), indicating the dominant role of emissions. It

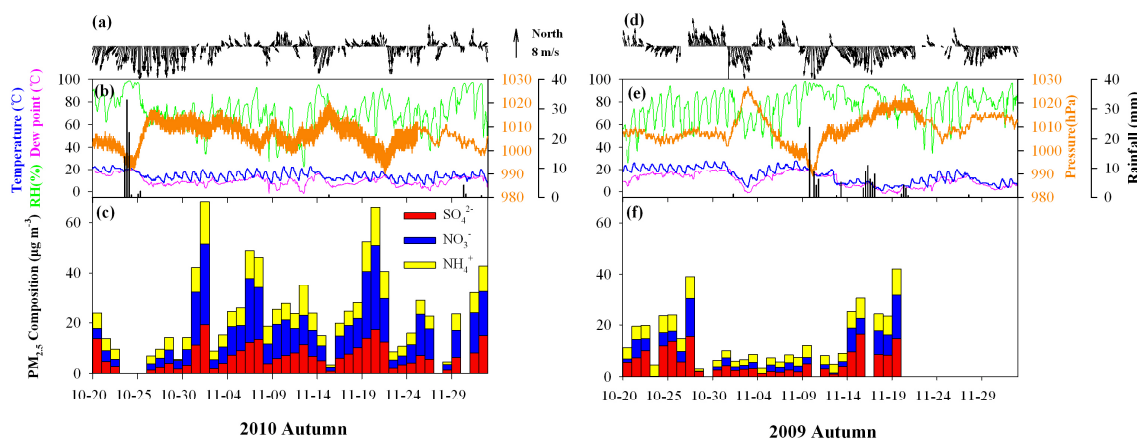


Fig. 8. Same as Fig. 4 but for the autumn of 2010 and 2009, respectively.

was noted that these pollution episodes were all associated with northeast winds from the ocean (Fig. 8a). Thus, this synoptic meteorology precluded the possibility of the long-range/regional transport from inland regions, which meant that local emission was the major source of pollution. Winds speeds during these SNA pollution episodes were relatively lower than those low pollution periods as shown in the figure. Also, relative humidity was usually higher. Those unfavorable meteorological conditions would surely contribute to the deterioration of air quality.

As we compare the same study period in the autumn of 2010 and 2009 (Fig. 8), air quality during the expo and post-expo period was completely different between the two years. During the expo, SNA was $12.2 \mu\text{g m}^{-3}$, about 25 % lower than the same period in 2009. Implementation of strict control measures and favorable meteorological conditions (e.g., higher wind speeds) were the major reasons. During the post-expo period, SNA averaged 28.8 ± 15.8 and $13.5 \pm 10.8 \mu\text{g m}^{-3}$ in 2010 and 2009, respectively. Over a 100 % increase of SNA in 2010 than in 2009 during the post-expo period clearly suggest the lifting of control measures was the main cause for the frequent occurrence of pollution episodes and poor air quality.

3.3.3 Pollution contributed from transported dust and local dust

On 12–13 November, another high pollution episode occurred as shown in Fig. 2. $\text{PM}_{2.5}$ far exceeded the criterion of $75 \mu\text{g m}^{-3}$ with the average concentration of $96.4 \mu\text{g m}^{-3}$, and PM_{10} reached the highest concentration of $398.1 \mu\text{g m}^{-3}$ during the whole study period. The mean $\text{PM}_{2.5}/\text{PM}_{10}$ ratio was as low as 0.24, indicating this pollution was caused by dust, again, similar as the pre-expo dust pollutant discussed in Sect. 3.1.1. A view from space helps to visualize the transport pathway of aerosol (Fig. S9) on 12 November. There was an obviously high AOD belt stretching from northern and eastern China out over the East China Sea and

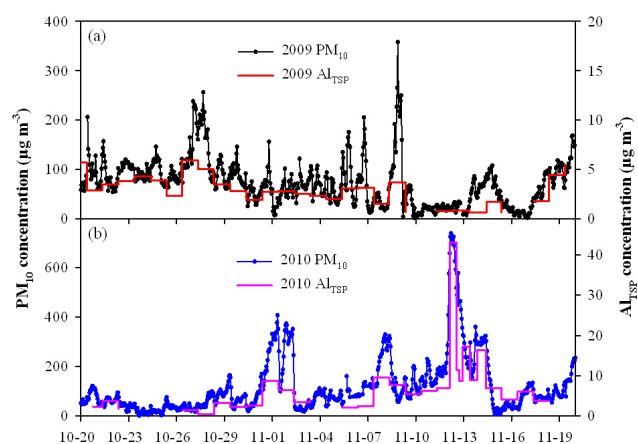


Fig. 9. Time series of hourly PM_{10} concentrations and daily Al concentrations in TSP (Al_{TSP}) during the autumn study period from 20 October to 19 November in 2009 (a) and 2010 (b), respectively.

Sea of Japan. Three-day back trajectories indicated that the source of aerosol originated from the Gobi Desert in Mongolia and Inner Mongolia. Compared to the pre-expo pollution event, this post-expo pollution event was evidently much stronger. Figure 9 plots the daily Al_{TSP} and the hourly PM_{10} concentrations, showing a very consistent variation of these two parameters. Between 02:00–13:00 LST on 12 November, PM_{10} showed its highest peak with an average concentration of $665.1 \mu\text{g m}^{-3}$, corresponding to the highest Al_{TSP} of $43.1 \mu\text{g m}^{-3}$. In this dust event, mineral aerosol accounted for a dominant fraction of 60 % in TSP.

During the normal times (i.e., excluding the dust invasion events), mineral aerosol in urban areas mainly derived from construction works and re-suspended dust. Comparison between 2010 and 2009 (Fig. 9) found out the temporal variation of Al_{TSP} varied relatively little in 2009 while it fluctuated much more intensively in 2010. For instance, the average Al_{TSP} from 20–30 October 2010 was at a relatively

low level of $2.21 \pm 1.05 \mu\text{g m}^{-3}$. Over the next two days, the daily Al_{TSP} increased 3–4 fold on 31 October and 1 November. Due to lifting of the short-term control measures during the expo, construction sites started to re-open as soon as the expo was announced to be closed (SEMC, 2011). Thus, the resumed construction activities also contributed to this pollution episode in addition to the enhanced traffic emission as stated in Sect. 3.3.1.

In order to quantitatively assess the impact from construction works, we calculated the concentrations of anthropogenic calcium, which could be used as a tracer for construction works in urban areas. The anthropogenic Ca concentration was calculated by removing its crustal source using Al as the tracer: $\text{Ca}_{\text{anthropogenic}} = \text{Ca}_{\text{total}} - \text{Al}_{\text{total}} \times (\text{Ca}/\text{Al})_{\text{crust}}$. The value of $(\text{Ca}/\text{Al})_{\text{crust}}$ is 0.5, which is the ratio of Ca vs. Al in crust. Based on this method, the average $\text{Ca}_{\text{anthropogenic}}$ concentration was 3.55 ± 1.25 and $3.03 \pm 1.92 \mu\text{g m}^{-3}$ during the expo period (20–30 October) and the post-expo period (31 October–20 November) in 2009, respectively. Obviously, no distinct difference between the two time frames was observed in 2009. In other words, the daily intensity of construction works was relatively stable. However, the situation was quite different in 2010. The average $\text{Ca}_{\text{anthropogenic}}$ concentration was 2.88 ± 1.85 and $6.98 \pm 3.19 \mu\text{g m}^{-3}$ during the Expo and post-expo (excluding the transported dust events), respectively. Anthropogenic Ca in 2010 during the expo was about 20 % lower than the same period in 2009, indicating the control measures on construction emissions were effective during the expo. However, anthropogenic Ca in 2010 during the post-expo increased by 140 % compared to during the expo and 130 % compared to the same period in 2009. More and more construction sites started to re-open after the expo, causing the increased emission of construction dust. Thus, the resumption of construction works after the expo and the easing of pollution controls was also one of the causes contributing to the rebound of poor air quality.

3.4 Comprehensive comparison between 2010 and 2009

3.4.1 Seasonal comparison of soluble ions between 2010 and 2009

Before we compare the differences of aerosol chemical composition between 2010 and 2009, it is necessary to evaluate if the meteorological conditions between these two years were distinctly different. Figure S10 shows the monthly mean values of the major meteorological parameters, i.e., temperature, dew point, wind speed, atmospheric pressure and monthly accumulated precipitation amount between 2009 and 2010. As shown in the figure, there were small differences between the two years for the first four parameters. As for temperature, the monthly difference (2010 minus 2009) during the expo was -1.4 , -1.8 , -0.1 , 2.5 , 0.6 , and -1.4 °C from May to October. As for dew point, wind speed and atmo-

spheric pressure, the monthly difference was within the range of $-1.7 \sim 1.8$ °C, $-0.5 \sim 0.5 \text{ m s}^{-1}$, and $-1.2 \sim 2.2$ mb, respectively. Compared to their absolute values, these differences could be considered as trivial. Monthly precipitation had the largest divergence between the two years due to its high variability in both spatial and temporal scales. The total rainfall amount during the expo in 2010 was 709.2 mm, about 14 % lower than that of the same period in 2009 (828.8 mm). Overall, we did not find very significant differences in the major meteorological conditions between 2009 and 2010. Hence, in regard of a long-term period (e.g., on a monthly or seasonal basis), the air quality should be mainly determined by the emission. Figure 10 compares the concentration levels of major soluble ions in $\text{PM}_{2.5}$ and TSP between 2010 and 2009 during the three seasons, respectively. The left panels compare the seasonal concentrations of each species and the right panels present the percentage changes of 2010 relative to 2009. The result of spring is shown in Fig. 10a and b. Significant decreases of SO_4^{2-} were observed in both $\text{PM}_{2.5}$ and TSP. Average SO_4^{2-} in $\text{PM}_{2.5}$ decreased from $7.9 \mu\text{g m}^{-3}$ in 2009 to $5.4 \mu\text{g m}^{-3}$ in 2010 with a reduction of 32 %. The decrease of SO_4^{2-} in TSP mainly came from its reduction in fine particles. Closing dirty and inefficient units of power plants and reducing the coal burning emission (UNEP, 2009) were the main causes for the reduction of particulate SO_4^{2-} . Opposite to SO_4^{2-} , NO_3^- in $\text{PM}_{2.5}$ increased from $6.2 \mu\text{g m}^{-3}$ in 2009 to $6.9 \mu\text{g m}^{-3}$ in 2010, indicating an increase of vehicle emission before and at the beginning of the expo. Of the cations, NH_4^+ , K^+ , and Ca^{2+} were found to have the most significant decreases. NH_4^+ in $\text{PM}_{2.5}$ decreased from $3.7 \mu\text{g m}^{-3}$ in 2009 to $3.1 \mu\text{g m}^{-3}$ in 2010. Since NH_4^+ was the major neutralization species for the acids, it was expected to decrease due to the significant decrease of SO_4^{2-} . K^+ , a typical tracer for biomass burning, showed about 30 % decreases in both $\text{PM}_{2.5}$ and TSP. Figure S11a and b show the spatial distribution of biomass burning carbon emission from FLAMBE (Reid et al., 2009) during spring of 2010 and 2009, respectively. It could be observed that the intensity of biomass burning diminished over the Yangtze River delta region in 2010 as compared to 2009. Banning of open field biomass burning as a special temporary control measure probably took effect during the beginning of the expo, and this could explain the lowered K^+ level. Ca^{2+} had the most significant decrease among all of the ions. Around a 69 % reduction of Ca^{2+} in TSP was achieved and should be due to the restriction of construction works and the frequent cleaning of traffic roads.

Figure 10c and d show the comparison results in summer. Similar to spring, control measures on SO_2 emission continued to take effect, resulting in about 15 % reduction of SO_4^{2-} compared to 2009. Also, increase of NO_3^- was evident, elevated from $4.5 \mu\text{g m}^{-3}$ in 2009 to $5.2 \mu\text{g m}^{-3}$ in 2010 in $\text{PM}_{2.5}$ and from 9.3 to $11.8 \mu\text{g m}^{-3}$ in TSP. A notable percentage of 15 and 27 % increases of NO_3^- in $\text{PM}_{2.5}$ and

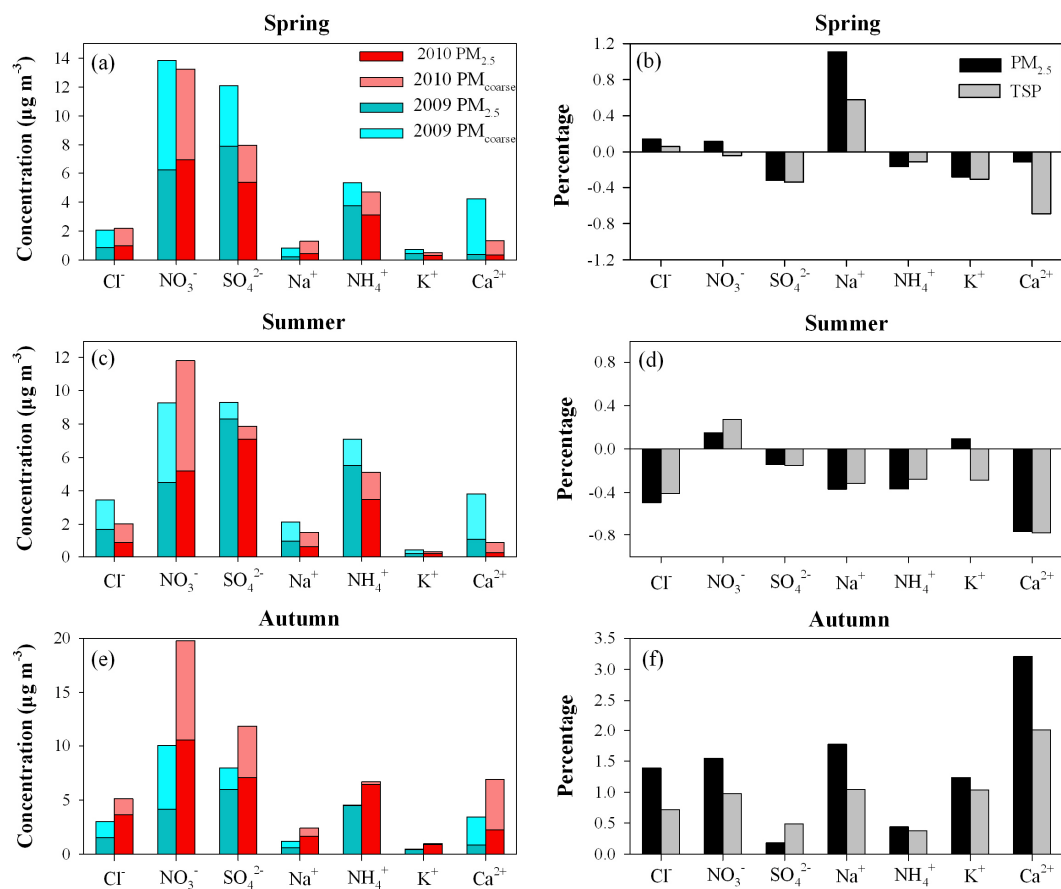


Fig. 10. (a, c, e) The seasonal average concentrations of Cl^- , NO_3^- , SO_4^{2-} , Na^+ , NH_4^+ , K^+ , and Ca^{2+} in $\text{PM}_{2.5}$ and TSP during 2009 and 2010. (b, d, f) The seasonal average percentage changes of the ions referred to above in 2010 relative to 2009.

TSP during summer suggested that more and more visitors came to the expo caused a substantial increase of vehicle emissions. NH_4^+ had 37 and 28 % reductions in $\text{PM}_{2.5}$ and TSP, respectively, as compared to 2009. On the one hand, the reduction of SO_4^{2-} offset the increase of NO_3^- . On the other hand, mean temperature in the summer of 2010 reached 31.1 °C, about 3.5 degrees higher than the same period in 2009. Higher temperature did not favor the formation of ammonium salts (e.g., NH_4NO_3 and $(\text{NH}_4)_2\text{SO}_4$) in the particulate phase and probably resulted in stronger depletion of NH_4^+ . Na^+ and Cl^- , which mainly derived from the marine source during summer in Shanghai (Huang et al., 2008), were found to decrease 30–50 % in 2010. As shown in Fig. S12a, wind in the summer of 2009 predominantly blew from the east, which is the open ocean of the East China Sea. While in the summer of 2010, winds shifted and mainly blew from the east to the south (counterclockwise) (Fig. S12b), where the impact from the marine source would be less important as continental outflows from Zhejiang Province and other continental regions would also contribute. Thus, the different transport pathways should be an important factor for the difference of marine aerosol levels and other pollutants. K^+ was

the only cation found to increase in $\text{PM}_{2.5}$. In Sect. 3.2, we have ascribed biomass burning to be a major source of pollution in summer. Comparison of the FLAMBE biomass burning carbon emissions in the summer of 2010 and 2009 further corroborated our measurement results as shown in Fig. S11c and d. Compared to 2009, biomass burning emission in 2010 was evidently more intense in Shanghai. As for the other parts of the Yangtze River delta, biomass burning in northern Zhejiang Province was most severe and evidently not well controlled. Via the prevailing south and southeast winds (Fig. S12b), Shanghai was probably impacted by the enhanced biomass burning from both local and regional transport. Ca^{2+} continued to have significant reductions of about 77 % in both $\text{PM}_{2.5}$ and TSP. Precipitation during the summer study period of 2010 was 149 mm, only half of that in 2009. Thus, stringent control measures on the construction works and road dust should be the major cause of decreased Ca^{2+} levels.

The comparison of results in the autumn study period were distinctly different from those of spring and summer. As shown in Fig. 10e and f, all the ion species unexceptionally increased in 2010 compared to 2009. Among the secondary

inorganic species, NO_3^- had the most significant enhancement. It increased over 1.5 fold from 4.1 to 10.5 $\mu\text{g m}^{-3}$ in $\text{PM}_{2.5}$, and almost onefold from 10.0 to 19.8 $\mu\text{g m}^{-3}$ in TSP. As stated in Sect. 3.3.3, the rebound of traffic emission during the post-expo period was the main cause for this. Compared to NO_3^- , SO_4^{2-} had a relatively lower increase of 18 % from 6.0 to 7.1 $\mu\text{g m}^{-3}$ in $\text{PM}_{2.5}$ and 48 % from 8.0 to 11.8 $\mu\text{g m}^{-3}$ in TSP. Due to increases of both NO_3^- and SO_4^{2-} , NH_4^+ also increased about 44 %. For the other ions, i.e., Cl^- , Na^+ , K^+ , and Ca^{2+} , their enhancements in $\text{PM}_{2.5}$ all exceeded 100 % while less in TSP. Especially, the increase of Ca^{2+} was most significant and only found in autumn, indicating the resumption of construction works and the re-suspended road dust due to more vehicle flow after the expo should be the cause for the enrichment of those crustal species.

3.4.2 Change of the relatively role of mobile source vs. stationary source

As discussed in the previous section, comparisons between 2010 and 2009 revealed that in the spring and summer phases of the expo, SO_4^{2-} had reductions while NO_3^- increased compared to 2009. In the autumn phase of the expo, although SO_4^{2-} and NO_3^- both showed an increase compared to 2009, the relative increasing percentage of NO_3^- was much higher than that of SO_4^{2-} . Thus, that raised the question: will NO_x emission become more important than SO_2 emission in the future of Shanghai? The ratio of $\text{NO}_3^-/\text{SO}_4^{2-}$ could be used as an indicator of the relative importance of mobile source vs. stationary source (Arimoto et al., 1996). Table 1 summarizes Shanghai's historic NO_3^- and SO_4^{2-} levels and the $\text{NO}_3^-/\text{SO}_4^{2-}$ ratios. During the early years, i.e., from 1999 to 2005, $\text{NO}_3^-/\text{SO}_4^{2-}$ ratios stayed in relatively low levels from 0.30 to 0.47 with occasional high values observed in the spring of 2005. Before 2005, air pollution in Shanghai was dominated by the stationary sources, e.g., power plants and industrial emission (Yao et al., 2002). As electricity in China was mainly produced from coal, and the flue-gas desulfurization (FGD) technology hadn't been implemented on most of the power plants, high emission of sulfur oxides was expected (UNEP, 2009). After 2005, obvious increase of the $\text{NO}_3^-/\text{SO}_4^{2-}$ ratios was observed compared to the early years. In 2006 and 2007, the ratios reached 0.71 and 0.67, respectively, almost twice that of the early years. During spring, summer, and autumn in 2009, the $\text{NO}_3^-/\text{SO}_4^{2-}$ ratios continued to rise to 0.78, 0.54, and 0.69, respectively. While in the same periods of 2010, the ratios were even more elevated to 1.3, 0.73, and 1.49, respectively. A comparison study of wet deposition between 2005 (rainwater) and 2009 (fog water) also showed a threefold increase of the $\text{NO}_3^-/\text{SO}_4^{2-}$ ratios (Table 1). For the first time, we found out the mass concentration of NO_3^- exceeded that of SO_4^{2-} in Shanghai during certain periods of the expo. This phenomenon was at-

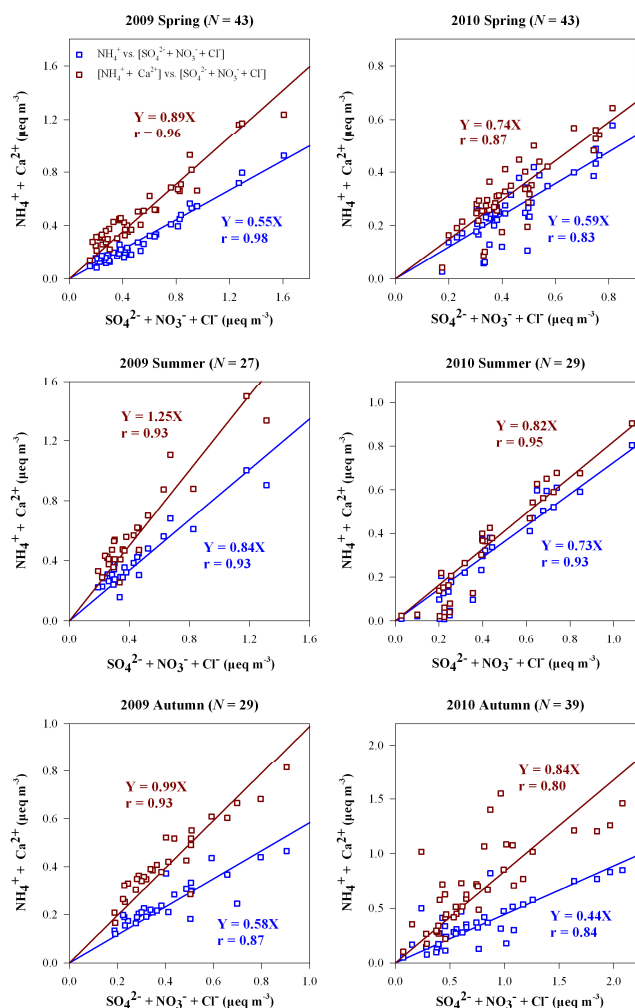


Fig. 11. Linear correlation between NH_4^+ and $[\text{SO}_4^{2-} + \text{NO}_3^- + \text{Cl}^-]$ and that between $[\text{NH}_4^+ + \text{Ca}^{2+}]$ and $[\text{SO}_4^{2-} + \text{NO}_3^- + \text{Cl}^-]$ in TSP during the three seasons in 2010 and 2009, respectively. All units are in units of equivalent concentrations ($\mu\text{eq m}^{-3}$). Linear regressions were forced through zero with correlation coefficients indicated in the figure.

tributed to two main causes. On the one hand, since 2006, more strict controls were implemented on the coal combustion emission, including reduction of the proportion of coal in the energy mix, close and/or replacement of inefficient and dirty coal-fired power plants, and installation of FGD devices for all the coal-fired stations of over 10 GW capacities in Shanghai. As a result, annual SO_4^{2-} concentrations had a significant decreasing trend as shown in the table. In the meanwhile, the annual growth rate of vehicle stocks of Shanghai reached over 12 % since 2000 (UNEP, 2009). NO_2 vertical column density from space over YRD continued to increase in the recent 5 yr (Wang and Tian, 2010). From the ground measurement results in Table 1, $\text{PM}_{2.5}$ nitrate also showed a slightly increasing trend. Thus, the change of

Table 1. Historical (and present study) concentrations of SO_4^{2-} and NO_3^- with the ratio of $\text{NO}_3^-/\text{SO}_4^{2-}$ in Shanghai.

Species	Year	Period	SO_4^{2-}	NO_3^-	$\text{NO}_3^-/\text{SO}_4^{2-}$	Reference
$\text{PM}_{2.5}$ ($\mu\text{g m}^{-3}$)	1999–2000	annual	15.2	6.5	0.43	Yao et al. (2002)
		1999	spring	12.6	5.4	0.43
	2005	summer	10.0	2.9	0.29	Wang et. (2006)
		autumn	13.6	5.1	0.38	
		spring	11.7	9.1	0.77	
		summer	5.4	2.6	0.48	
		autumn	8.7	3.7	0.43	
		winter	15.8	7.1	0.45	
		winter	9.6	6.8	0.71	
	2006	spring	10.6	7.1	0.67	Huang et al. (2010)
	2009	spring	7.9	6.2	0.79	Huang et al. (2012a)
		summer	8.3	4.5	0.54	This work
	2010	autumn	6.0	4.1	0.69	This work
spring		5.4	6.9	1.29		
summer		7.1	5.2	0.73		
Rainfall ($\mu\text{eq L}^{-1}$)	2005	annual	199.6	49.8	0.32	Huang et al. (2008)
Fog ($\mu\text{eq L}^{-1}$)	2009–2010	annual	2830.0	2416.0	1.10	Li et al. (2011)

emission sources is reflected in the increased $\text{NO}_3^-/\text{SO}_4^{2-}$ ratios. Due to the expansion of the transportation system, NO_x emissions were projected to increase by 60–70 % by 2020 (Chen et al., 2006), suggesting that nitrogen emission had the potential to be the prior pollutant in megacities of China.

3.4.3 Implications for soil components (Ca^{2+}) reduction

In Sect. 3.4.1, we found out that Ca^{2+} had the most obvious changes in 2010 compared to 2009. Ca^{2+} was another important neutralizer for buffering the acids other than NH_4^+ , and it mainly existed in the form of CaSO_4 , $\text{Ca}(\text{NO}_3)_2$, and CaCl_2 in Shanghai (Wang et al., 2006). In order to evaluate the impact of the change of soil components on the aerosol formation, we plot the linear correlations between NH_4^+ and $[\text{SO}_4^{2-} + \text{NO}_3^- + \text{Cl}^-]$ and also that between $[\text{NH}_4^+ + \text{Ca}^{2+}]$ and $[\text{SO}_4^{2-} + \text{NO}_3^- + \text{Cl}^-]$ in TSP during the three seasons in 2010 and 2009, respectively (Fig. 11). All the ions are in units of equivalent concentrations ($\mu\text{eq m}^{-3}$). As shown in the figure, NH_4^+ and $[\text{NH}_4^+ + \text{Ca}^{2+}]$ both had significant linear correlations with $[\text{SO}_4^{2-} + \text{NO}_3^- + \text{Cl}^-]$. The regressions were all forced through zero, so the neutralization extent of Ca^{2+} and NH_4^+ on acids could be quantified by the slopes of NH_4^+ vs. $[\text{SO}_4^{2-} + \text{NO}_3^- + \text{Cl}^-]$ and $[\text{NH}_4^+ + \text{Ca}^{2+}]$ vs. $[\text{SO}_4^{2-} + \text{NO}_3^- + \text{Cl}^-]$, respectively. It is found that during the same season in both years, the neutralization ability of NH_4^+ on acids did not vary distinctly. For instance, the slope of NH_4^+ vs. $[\text{SO}_4^{2-} + \text{NO}_3^- + \text{Cl}^-]$ during the spring of 2009 and 2010 was 0.55 and 0.59. During summer it was 0.84 and 0.73, and during winter, it was 0.58 and 0.44. However, we found a big discrepancy of the $[\text{NH}_4^+ + \text{Ca}^{2+}]/[\text{SO}_4^{2-} + \text{NO}_3^-$

+ $\text{Cl}^-]$ slopes between 2009 and 2010. In general, the $[\text{NH}_4^+ + \text{Ca}^{2+}]/[\text{SO}_4^{2-} + \text{NO}_3^- + \text{Cl}^-]$ slopes in 2010 were lower than those in 2009. If we subtract $\text{NH}_4^+ / [\text{SO}_4^{2-} + \text{NO}_3^- + \text{Cl}^-]$ slopes from $[\text{NH}_4^+ + \text{Ca}^{2+}]/[\text{SO}_4^{2-} + \text{NO}_3^- + \text{Cl}^-]$ slopes, the neutralization extent of Ca^{2+} on the acids could be estimated. It was calculated that the neutralization percentage of Ca^{2+} on acids during spring and summer in 2009 was 33 and 16 %, respectively. While it reduced to 14 and 9 % during the 2010 expo, respectively. As stated previously, the temporary shut down of construction works and cleansing of the main traffic roads during the expo had effectively lowered the soil dust concentrations. Due to this special measure, the effect of mineral dust on the acid neutralization was depressed and hence reduced the aerosol concentration, especially of coarse particles. The only exception was found in autumn. As shown in Fig. 10e and f, no obvious difference of the discrepancy of the two slopes between the two years was observed. The neutralization percentage of Ca^{2+} on acids during the autumn of 2009 and 2010 was calculated as 41 and 40 %, respectively. As discussed in Sects. 3.3.3 and 3.4.1, the resumption of construction sites and re-suspended road dust after the expo caused an elevation of mineral aerosol and buffered more acids to form secondary aerosol. While during the spring and summer of 2010, when control measures were implemented, it was estimated that the neutralization of Ca^{2+} on acids had been reduced by about 7–17 % compared to 2009, which implied that reducing the mineral aerosol could also be beneficial for the alleviation of air pollution in megacities of China.

4 Conclusions

We conducted three air quality campaigns before, during, and after the 2010 World Expo in Shanghai. Trace gases, aerosol chemical components, and major meteorological factors were measured. The results showed the response of secondary aerosol components to both the control measures and the human activities during the expo. In spring, the most severe pollution episode was caused by a floating dust originating from northwestern China on 26–28 April, right before the opening of the expo. A comparison to the similar period of 2009 found that floating dust was a common phenomenon impairing the air quality of eastern China in spring. A significant increasing trend of SNA (SO_4^{2-} , NO_3^- , and NH_4^+) concentrations was observed from 22 April to 2 May, which was attributed to the enhanced human activities as the expo was approaching. Nitrate had the most significant daily increasing rate of $1.1 \mu\text{g m}^{-3} \text{d}^{-1}$ due to enhanced vehicle emission. In summer, two intensive pollution episodes were found to be a mixed pollution of SNA with biomass burning due to loose control of post-harvest straw burning. In the autumn phase of the expo, before the closing of the expo (20 to 30 October), the air quality over Shanghai was much better than ever before. However, the air quality rapidly plummeted as soon as the expo was announced closed. SNA increased 3–6 fold to be 42.1 and $68.2 \mu\text{g m}^{-3}$ on 31 October and 1 November, respectively, as compared to 20–30 October. Of which, nitrate increased most ~ 5 –8 fold, indicating the serious impact from enhanced vehicle emission. The anthropogenic Ca as a tracer from construction dust increased from $2.88 \pm 1.85 \mu\text{g m}^{-3}$ during the expo to $6.98 \pm 3.19 \mu\text{g m}^{-3}$ during the post-expo period, attributed to the resumption of construction works after the expo. No successive control measures and loose regulations after the expo were responsible for this jump to bad quality.

Compared to the spring and summer of 2009, NO_3^- increased 12–15 % while SO_4^{2-} showed reductions of 15–30 % in 2010. Continuous desulfurization of SO_2 emission from power plants in recent years was responsible for the lowered SO_4^{2-} , while enhanced traffic emission due to tremendous number of expo visitors was the major contributor to the increased NO_3^- . Compared to the autumn in 2009, all the ion components increased in 2010 owing to the lifting of emission control measures after the expo. SO_4^{2-} was found to have a lower increase while NO_3^- had a significant increase of 150 %. For the first time, we found out the mass concentration of NO_3^- exceeded that of SO_4^{2-} in Shanghai during certain periods of the expo. Reducing NO_x emission will be China's priority in the future in order to improve the air quality over the megacity. In spring and summer, Ca^{2+} had the most significant reduction among all the ions. Prohibition of construction works and frequent cleaning of the traffic roads were testified as effective in lowering the mineral aerosol levels. The neutralization ability of Ca^{2+} on acids was estimated

to decrease by 7–17 %. However, the resumption of construction works and enhanced traffic flows after the expo made Ca^{2+} gain a tremendous increase of 320 %. It was suggested that controlling the emission of mineral aerosol was also beneficial for the alleviation of air pollution in China.

During the 2010 expo, apparent improvement of air quality was achieved, which was attributed to that the Shanghai municipal government has implemented a series of control strategies including stepwise, long-term, region-wide and emergency measures (Table S1). The growth of total energy consumption for the industrial, transport and building sectors was controlled and the energy efficiency had improved a lot. Use of natural gas, installation of wind power facilities and imported electricity from neighboring provinces (e.g., Anhui Province, and electricity generated by the Three Gorges Hydropower Station) resulted in less coal combustion (UNEP, 2009). Some strict emission control measures, e.g., emission control from power plants, vehicle flows, and ban of burning straws, did take effect during the expo. However, this kind of strict emission control measures did not last long, and it was only given to a specific event in China, such as the Beijing Olympic Games (Zhang et al., 2009), the Shanghai Expo, and the Guangzhou Asian Games (Liu et al., 2012). We suggest that the government should abandon the short-sighted attitude of only considering some specific events. Instead, a long-term effort is required for the improvement and sustainability of air quality in megacities of China.

Supplementary material related to this article is available online at: <http://www.atmos-chem-phys.net/13/5927/2013/acp-13-5927-2013-supplement.zip>.

Acknowledgements. This work was supported by National Natural Science Foundation of China (Grant Nos. 41128005 (fund for collaboration with overseas scholars), 21277030, 20977017), Shanghai environmental protection science and development funding (No. 2011-55), and the great international collaboration project of MOST, China (2010DFA92230).

Edited by: K. Schaefer

References

- Arimoto, R., Duce, R. A., Savoie, D. L., Prospero, J. M., Talbot, R., Cullen, J. D., Tomza, U., Lewis, N. F., and Jay, B. J.: Relationships among aerosol constituents from Asia and the North Pacific during PEM-West A, *J. Geophys. Res.*, 101, 2011–2023, 1996.
- CAI-Asia: Clean Air Initiative for Asian Cities (CAI-Asia) Center, Blue Skies at Shanghai EXPO 2010 and Beyond: Analysis of Air Quality Management in Cities with Past and Planned Mega-Events, A Survey Report, 2009.
- CAI-Asia: Clean Air Initiative for Asian Cities (CAI-Asia) Center, Blue Skies Shanghai EXPO 2010 and Beyond: 3rd Shanghai Clean Air Forum & International Workshop Achievement

- of 2010 EXPO Air Quality Management, Post-EXPO Workshop Report, 2011.
- Chen, C. H., Wang, B. Y., Fu, Q. Y., Green, C., and Streets, D. G.: Reductions in emissions of local air pollutants and co-benefits of Chinese energy policy: a Shanghai case study, *Energ. Policy*, 34, 754–762, 2006.
- Fu, Q. Y., Zhuang, G. S., Wang, J., Xu, C., Huang, K., Li, J., Hou, B., Lu, T., and Streets, D. G.: Mechanism of formation of the heaviest pollution episode ever recorded in the Yangtze River Delta, China, *Atmos. Environ.*, 42, 9, 2023–2036, 2008.
- Hao, N., Valks, P., Loyola, D., Cheng, Y. F., and Zimmer, W.: Space-based measurements of air quality during the World Expo 2010 in Shanghai, *Environ. Res. Lett.*, 6, 044004, doi:10.1088/1748-9326/6/4/044004, 2011.
- Huang, K., Zhuang, G., Lin, Y., Fu, J. S., Wang, Q., Liu, T., Zhang, R., Jiang, Y., Deng, C., Fu, Q., Hsu, N. C., and Cao, B.: Typical types and formation mechanisms of haze in an Eastern Asia megacity, Shanghai, *Atmos. Chem. Phys.*, 12, 105–124, doi:10.5194/acp-12-105-2012, 2012a.
- Huang, K., Zhuang, G., Lin, Y., Wang, Q., Fu, J. S., Zhang, R., Li, J., Deng, C., Jiang, Y., and Fu, Q.: Impact of anthropogenic emission on air-quality over a megacity – revealed from an intensive atmospheric campaign during the Chinese Spring Festival, *Atmos. Chem. Phys.*, 12, 11631–11645, doi:10.5194/acp-12-11631-2012, 2012b.
- Huang, K., Zhuang, G. S., Li, J. A., Wang, Q. Z., Sun, Y. L., Lin, Y. F., and Fu, J. S.: Mixing of Asian dust with pollution aerosol and the transformation of aerosol components during the dust storm over China in spring 2007, *J. Geophys. Res.*, 115, D00K13, doi:10.1029/2009JD013145, 2010.
- Huang, K., Zhuang, G. S., Xu, C., Wang, Y., and Tang, A. H.: The chemistry of the severe acidic precipitation in Shanghai, China, *Atmos. Res.*, 89, 149–160, 2008.
- Huang, X. F., He, L. Y., Xue, L., Sun, T. L., Zeng, L. W., Gong, Z. H., Hu, M., and Zhu, T.: Highly time-resolved chemical characterization of atmospheric fine particles during 2010 Shanghai World Expo, *Atmos. Chem. Phys.*, 12, 4897–4907, doi:10.5194/acp-12-4897-2012, 2012c.
- Li, P. F., Li, X., Yang, C. Y., Wang, X. J., Chen, J. M., and Collett, J.: Fog water chemistry in Shanghai, *Atmos. Environ.*, 45, 4034–4041, 2011.
- Lin, Y., Huang, K., Zhuang, G., Fu, J. S., Xu, C., Shen, J., and Chen, S.: Air quality over the Yangtze River Delta during the 2010 Shanghai Expo, *Aerosol Air Qual. Res.*, in press, 2013.
- Liu, H., Wang, X. M., Zhang, J. P., He, K. B., Wu, Y., Xu, J. Y.: Emission controls and changes in air quality in Guangzhou during the Asian Games, *Atmos. Environ.*, in press, doi:10.1016/j.atmosenv.2012.08.004, 2012.
- Malm, W. C., Sisler, J. F., Huffman, D., Eldred, R. A., and Cahill, T. A.: Spatial and Seasonal Trends in Particle Concentration and Optical Extinction in the United-States, *J. Geophys. Res.*, 99, 1347–1370, 1994.
- Reid, J. S., Hyer, E. J., Prins, E. M., Westphal, D. L., Zhang, J. L., Wang, J., Christopher, S. A., Curtis, C. A., Schmidt, C. C., Eleuterio, D. P., Richardson, K. A., and Hoffman, J. P.: Global Monitoring and Forecasting of Biomass-Burning Smoke: Description of and Lessons From the Fire Locating and Modeling of Burning Emissions (FLAMBE) Program, Selected Topics in Applied Earth Observations and Remote Sensing, *IEEE J. Sel. Top. Appl.*, 2, 144–162, 2009.
- SEMC: Shanghai Environmental Monitoring Center, Joint monitoring and follow up assessment on air quality of the 2010 Shanghai Expo. Workshop for the regional air quality over the Yangtze River Delta, Shanghai, China, 22 November, 2011.
- SEPB: Shanghai Environment Protection Bureau, available at: <http://www.sepb.gov.cn/fa/cms/shhj/shhj2272/shhj2159/2010/04/20669.htm> (last access: 18 June 2013), (in Chinese), 2010.
- SMSB: Shanghai Municipal Statistics Bureau, Shanghai sixth national census in 2010 Communiqué on Major Data, Shanghai Municipal Statistics Bureau, available at: <http://www.shanghai.gov.cn/shanghai/node2314/node2319/node12344/u26ai25463.html> (last access: 18 June 2013), (in Chinese), 2011.
- Sun, Y., Zhang, Q., Macdonald, A. M., Hayden, K., Li, S. M., Liggio, J., Liu, P. S. K., Anlauf, K. G., Leaitch, W. R., Steffen, A., Cubison, M., Worsnop, D. R., van Donkelaar, A., and Martin, R. V.: Size-resolved aerosol chemistry on Whistler Mountain, Canada with a high-resolution aerosol mass spectrometer during INTEX-B, *Atmos. Chem. Phys.*, 9, 3095–3111, doi:10.5194/acp-9-3095-2009, 2009.
- Sun, Y., Zhuang, G. S., Yuan, H., Zhang, X. Y., and Guo, J. H.: Characteristics and sources of 2002 super dust storm in Beijing, *Chinese Sci. Bull.*, 49, 698–705, 2004.
- UNEP: United Nations Environment Programme, UNEP Environmental Assessment Expo 2010 Shanghai, China, available at: http://www.unep.org/pdf/SHANGHAI-REPORT_FullReport.pdf, 2009.
- USEPA: Quality assurance handbook for air pollution measurement systems, EPA-454/R-98-004, US Environmental Protection Agency, Office of Air Quality Planning and Standards, Air Quality Assessment Division, Research Triangle Park, NC, USA, 1998.
- Wang, L. and Tian, Q. J.: Spatio-temporal distribution of tropospheric NO₂ and quantitative analysis of its impact factors over Yangtze Delta based on OMI satellite measurements, 2010 18th International Conference on Geoinformatics, 1–5, doi:10.1109/GEOINFORMATICS.2010.5567650, 2010.
- Wang, T., Nie, W., Gao, J., Xue, L. K., Gao, X. M., Wang, X. F., Qiu, J., Poon, C. N., Meinardi, S., Blake, D., Wang, S. L., Ding, A. J., Chai, F. H., Zhang, Q. Z., and Wang, W. X.: Air quality during the 2008 Beijing Olympics: secondary pollutants and regional impact, *Atmos. Chem. Phys.*, 10, 7603–7615, doi:10.5194/acp-10-7603-2010, 2010.
- Wang, Y., Hao, J., McElroy, M. B., Munger, J. W., Ma, H., Chen, D., and Nielsen, C. P.: Ozone air quality during the 2008 Beijing Olympics: effectiveness of emission restrictions, *Atmos. Chem. Phys.*, 9, 5237–5251, doi:10.5194/acp-9-5237-2009, 2009.
- Wang, Y., Zhuang, G. S., Tang, A. H., Zhang, W. J., Sun, Y. L., Wang, Z. F., and An, Z. S.: The evolution of chemical components of aerosols at five monitoring sites of China during dust storms, *Atmos. Environ.*, 41, 1091–1106, 2007.
- Wang, Y., Zhuang, G. S., Zhang, X. Y., Huang, K., Xu, C., Tang, A. H., Chen, J. M., and An, Z. S.: The ion chemistry, seasonal cycle, and sources of PM_{2.5} and TSP aerosol in Shanghai, *Atmos. Environ.*, 40, 2935–2952, 2006.
- Yang, S. J., He, H. P., Lu, S. L., Chen, D., and Zhu, J. X.: Quantification of crop residue burning in the field and its influence on ambient air quality in Suqian, China, *Atmos. Environ.*, 42, 1961–

- 1969, 2008.
- Yao, X. H., Chan, C. K., Fang, M., Cadle, S., Chan, T., Mulawa, P., He, K. B., and Ye, B. M.: The water-soluble ionic composition of PM_{2.5} in Shanghai and Beijing, China, *Atmos. Environ.*, 36, 4223–4234, 2002.
- Ye, B. M., Ji, X. L., Yang, H. Z., Yao, X. H., Chan, C. K., Cadle, S. H., Chan, T., and Mulawa, P. A.: Concentration and Chemical Composition of PM_{2.5} in Shanghai for a 1-year Period. *Atmos. Environ.*, 37, 499–510, 2003.
- Yuan, H., Wang, Y., and Zhuang, G. S.: Simultaneous determination of organic acids, methanesulfonic acid and inorganic anions in aerosol and precipitation samples by ion chromatography, *J. Instr. Anal.*, 22, 11–44, 2003.
- Zhang, X. Y., Wang, Y. Q., Lin, W. L., Zhang, Y. M., Zhang, X. C., Gong, S., Zhao, P., Yang, Y. Q., Wang, J. Z., Hou, Q., Zhang, X. L., Che, H. Z., Guo, J. P., and Li, Y.: Changes of Atmospheric Composition and Optical Properties over Beijing 2008 Olympic Monitoring Campaign, *B. Am. Meteorol. Soc.*, 90, 1633–1651, doi:10.1175/2009BAMS2804.1, 2009.
- Zhuang, G. S., Guo, J. H., Yuan, H., and Zhao, C. Y.: The compositions, sources, and size distribution of the dust storm from China in spring of 2000 and its impact on the global environment, *Chinese Sci. Bull.*, 46, 895–901, 2001.